Investigating the γ decay of ^{65}Ni from particle-γ coincidence data

L. Crespo Campo,[1,*] A. C. Larsen,[1] F. L. Bello Garrote,[1] T. K. Eriksen,[2] F. Giacoppo,[3,4] A. Görgen,[1] M. Guttormsen,[1] M. Klintefjord,[1] T. Renstrøm,[1] E. Sahin,[1] S. Siem,[1] T. G. Tornyi,[2] and G. M. Tveten[1]

[1]*Department of Physics, University of Oslo, N-0316 Oslo, Norway*

[2]*Department of Nuclear Physics, Research School of Physics and Engineering, The Australian National University, Acton, ACT 2601, Australia*

[3]*Helmholtz Institute Mainz, 55099 Mainz, Germany*

[4]*GSI Helmholtzzentrum für Schwerionenforschung GmbH, 64291 Darmstadt, Germany*

(Received 6 March 2017; published 18 July 2017)

The γ decay of ^{65}Ni has been studied from particle-γ coincidence data on the ^{64}Ni$(d,p\gamma)^{65}$Ni reaction. γ-ray spectra at excitation energies below $E_x \approx 2$ MeV have been studied and compared with previous measurements. Coincidences corresponding to $E_x \approx 4.4$–6.1 MeV have been used to constrain the shape of the nuclear level density and γ-strength function of ^{65}Ni by means of the Oslo method. The experimental γ-strength function presents an enhancement at γ energies below $E_\gamma \approx 3$ MeV. In addition, a resonance-like structure centered at $E_\gamma \approx 4.6$ MeV is seen together with accumulated strength at $E_\gamma \approx 2.6$–3.6 MeV. The obtained results contribute to the systematic study of γ decay in the Ni isotopes, which is of great interest for the understanding of both single-particle and collective nuclear structure phenomena.

DOI: 10.1103/PhysRevC.96.014312

I. INTRODUCTION

In recent years much effort has been directed to the study of the Ni isotopes. Both experimental and theoretical works have given insight into complex nuclear structure phenomena, involving single-particle [1] and collective [2] excitations. The Ni isotopic chain extends from $A = 48$ to $A = 79$, covering a wide range of neutron separation energies and including the $Z = 28$ and $N = 28,50$ shell closures [3]. The proton shell closure at $Z = 28$ tends to stabilize the spherical shape of the ground state between ^{56}Ni and ^{78}Ni. As a result, their level structure at low spins is reasonably well described with shell-model calculations, in which low-energy excitations are mostly determined by the neutrons filling the $p_{3/2}$, $f_{5/2}$, $p_{1/2}$, and $g_{9/2}$ orbitals [4,5]. At higher spins, rotational bands have been measured in $^{56-63}$Ni [6–11], including highly deformed and even superdeformed bands in ^{56,57}Ni [7,12].

Further, the experimental results for ^{68}Ni indicate the presence of a subshell closure at $N = 40$ [13–16], although shell model calculations estimate a rather small ($\approx$2 MeV) gap allowing for cross-shell excitations at low and moderate spins [17]. In addition, recent measurements supported by Monte Carlo shell model calculations suggest a triple-shape coexistence [18,19], also expected for ^{70}Ni [20,21].

The experimental study of γ decay in the Ni isotopes has been a fundamental tool for the understanding of both single-particle and collective excitations [6–12]. Measurements of the γ-strength function (γSF), or average reduced γ-transition probability [22], have increased our knowledge on statistical γ decay and γ resonances [23], present in various Ni isotopes. The results for ^{60}Ni indicate accumulations of $M1$ excited spin-1 states near $E_x = 8$ MeV and $E_x = 9$ MeV, identified as isoscalar and isovector $M1$ resonances dominated by proton and neutron $f_{7/2} \rightarrow f_{5/2}$ spin-flip excitations [24]. In addition, results from Ref. [25] also indicate the presence of resonances with a significant $M1$ component at $E_\gamma \approx 9$–14 MeV in ^{58,60,62}Ni. Moreover, a strong $E1$ pygmy resonance, often described as being due to the oscillation of the neutron skin with respect to an $N \approx Z$ core [26,27], has been seen in ^{68}Ni at $\approx$9.6 MeV [28,29].

One of the least explored features observed in the γSF is the low-energy enhancement, or increased probability of γ decay with energies below $\approx$2–4 MeV. This low-energy enhancement or *upbend* has been seen in a wide mass range of nuclei, including ^{60,64}Ni [30–41]. The physical mechanisms underlying this upbend are still not well understood, and theoretical investigations propose different interpretations. While calculations within the quasiparticle random phase approximation predict an $E1$ character of the upbend in ^{94,96,98}Mo [42], shell model calculations for $^{94-96}$Mo and ^{90}Zr indicate a strong enhancement for low γ-energy $M1$ transitions due to the recoupling of high-j nucleon orbits [43]. The results are supported by large-basis shell-model calculations on ^{56,57}Fe [44], indicating a large increase in the $M1$ strength for low γ-ray energies, dominated by 0 $\hbar\omega$ transitions within the $f_{7/2}$ shell. In addition, two-step cascade measurements have confirmed the $M1$ character of the upbend in ^{60}Ni [40].

A large amount of the experimental information on this upbend has been obtained from particle-γ coincidence measurements analyzed with the Oslo method [45–48]. This technique, developed by the nuclear physics group at the University of Oslo, allows for the simultaneous extraction of the nuclear level density (NLD) and γSF. The application of the Oslo method led to the experimental discovery of the upbend, first seen in ^{56,57}Fe [30]. Later, it was used to prove the presence of an upbend in nuclei such as $^{43-44}$Sc [34,35], ^{50,51}V [36], and ^{64}Ni [37], among others. Recently, variations of the Oslo method have allowed for the study of the NLD and γSF in more neutron-rich nuclei via the analysis of experimental data

*l.c.campo@fys.uio.no

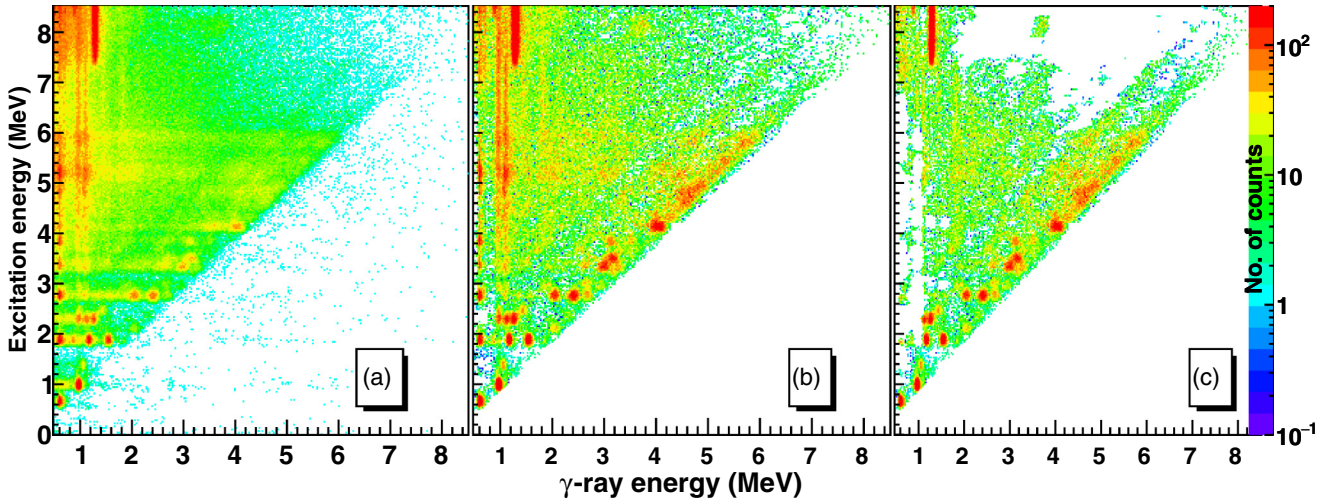

FIG. 1. Original (a), unfolded (b), and first-generation (c) coincidence matrices for ^{65}Ni from the ^{64}Ni$(d,p\gamma)^{65}$Ni reaction. The x axis represents the γ energy while the y axis gives the excitation energy of ^{65}Ni. The number of counts is represented by the color scale.

from nuclear β decay [49] and reactions on inverse kinematics [50]. As a result, the γSF of nuclei such as ^{70}Ni have been obtained, also displaying a low-energy enhancement [51]. The study of progressively more neutron-rich Ni isotopes in this mass region is therefore of great importance to understand the systematic evolution of the upbend with features such as nuclear mass, N/Z ratio, or nuclear deformation.

In this work, the γ decay of ^{65}Ni has been studied from particle-γ coincidence data on the ^{64}Ni$(d,p\gamma)^{65}$Ni reaction. γ-ray spectra have been obtained at excitation energies below $E_x \approx 4$ MeV, allowing for the identification of a transition not tabulated in Ref. [52]. Data at $E_x \approx 4.4$–6.1 MeV have been analyzed with the Oslo method to constrain the shape of the NLD and γSF of ^{65}Ni. The presence of an upbend and resonance-like structures in the γSF is presented and their possible origin discussed. Finally, the results will be compared to experimental data on neighboring nuclei.

This article is organized as follows: in Sec. II the experimental details and data analysis are summarized, and the performance of the Oslo method in the present case is discussed. In Sec. III the normalization procedure of the NLD and γSF is described. A deeper study of the γ decay of ^{65}Ni is given in Sec. IV. Further, in Sec. V the obtained results are discussed and compared with other experimental data. Finally, a summary and outlook are given in Sec. VI.

II. EXPERIMENTAL DETAILS AND THE OSLO METHOD

The experiment was performed at the Oslo Cyclotron Laboratory (OCL) using a 12.5 MeV deuteron beam with typical currents of 0.2–0.3 nA. A 99% enriched ^{64}Ni self-supporting target of 1 mg/cm^2 thickness was used and particle-γ coincidences were measured during 3 days in order to study the ^{64}Ni$(d,p\gamma)^{65}$Ni reaction.

The emitted charged particles were measured with the Silicon Ring (SiRi) particle-detector array [53]. The SiRi array is formed by eight telescope ΔE-E silicon detectors, each of them consisting on a 130-μm thin layer positioned in front of a 1550-μm thick back detector. Since each of the thin detectors are segmented in eight strips, the angles of the emitted charged particles can be detected with an angular resolution of $\Delta\theta = 2^\circ$, with a solid angle coverage of $\approx$6%. For this experiment, the SiRi detector system was placed in backward angles with respect to the beam direction, covering scattering angles from 126° to 140° in the laboratory frame. The emitted γ rays were measured with the CACTUS array [54], consisting of 26 collimated 5″ × 5″ NaI(Tl) detectors with a 14.1(1)% efficiency at $E_\gamma = 1332.5$ keV. The ejected charged particles and emitted γ rays were then measured in coincidence with a time resolution (FWHM) of $\approx$15 ns. The energy resolution for SiRi is $\approx$130 keV at 692 keV and the resolution for CACTUS is $\approx$70 keV at 1017 keV.

Using the SiRi array, the energy loss of the ejected charged particles in the thin (ΔE) and thick (E) detectors was measured. From the ΔE-E curves, the various charged particle species were identified, i.e, the different reaction channels distinguished. By setting a gate on the ejected protons, the (d,p) reaction channel was selected. From the measured energies of the emitted charged particles and the kinematics of the reaction, the corresponding excitation energies of the final nucleus ^{65}Ni could be obtained. As a result, the γ rays emitted by ^{65}Ni from a given excitation energy could be measured and a coincidence matrix was obtained, as shown in Fig. 1(a). This coincidence matrix displays the number of counts registered for a given excitation energy E_x and γ energy E_γ and it is therefore directly connected to the probability of nuclear γ decay $P(E_x, E_\gamma)$. The coincidence matrix shown in Fig. 1(a) is the starting of point for the Oslo method, which consists on three main steps: (i) unfolding, (ii) extraction of first-generation (primary) γ rays,[1] and (iii) extraction and normalization of the NLD and γSF.

Applying an iterative procedure [45], the γ-ray spectra were corrected for the response of the detectors in CACTUS (unfolded). The applied response functions and detector

[1]The first γ rays emitted in the decay cascades.

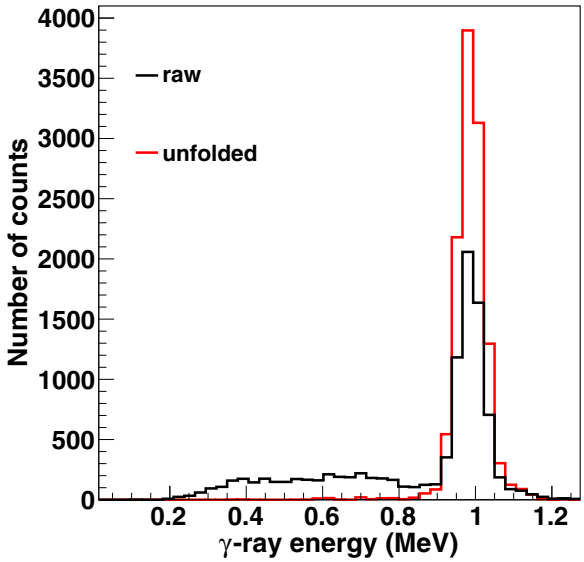

FIG. 2. Comparison between raw and unfolded γ-ray spectra from $E_x = 1.017$ MeV.

efficiencies were obtained in 2012 from in-beam γ lines listed in Ref. [37]. The resulting unfolded matrix is shown in Fig. 1(b). To demonstrate the quality of the unfolding technique, a comparison between the raw and the unfolded γ-ray spectra at $E_x \simeq 1.0$ MeV is shown in Fig. 2. A single peak at $E_\gamma = 1.017$ MeV is seen in the unfolded spectra, corresponding to the only transition seen from the fourth excited state of ^{65}Ni at $E_x = 1.017$ MeV. The component from Compton scattering, seen in the raw spectra, has been successfully removed through the unfolding procedure. It should be noted that no artificial fluctuations are introduced with this unfolding technique, which preserves the experimental statistical uncertainties.

From the unfolded γ-ray spectra, the distribution of primary γ rays was obtained for each excitation energy bin by means of an iterative subtraction technique described in Ref. [46]. The main assumption of this procedure is that the γ-decay routes from a given excitation energy are independent of whether it was directly populated in the reaction, or through γ decay from above-lying states (see Ref. [48] for a discussion of the uncertainties regarding this subtraction technique). The resulting matrix (primary γ-ray matrix) is shown in Fig. 1(c). In addition, the effect of the extraction of primary spectra is illustrated in Fig. 3, in which a section of the unfolded and first-generation coincidence matrices are compared. The peaks marked with a $\star$ correspond to secondary transitions, successfully removed in the extraction of first-generation γ rays.

From the primary γ-ray coincidence matrix, the functional form of the NLD and the γ-transmission coefficient was obtained by means of the iterative procedure described in Ref. [47]. The main underlying assumption of this method is that the considered γ-decay process is statistical; i.e, the studied reaction has populated a compound state which decays independently on how it was formed [1]. Then, the following relation holds:

$$P(E_\gamma, E_x) \propto \rho(E_f)\mathcal{T}(E_\gamma), \tag{1}$$

where $P(E_\gamma, E_x)$ is the experimental primary coincidence matrix, $\rho(E_f)$ is the NLD at the final excitation energy E_f, with $E_f = E_x - E_\gamma$, and $\mathcal{T}$ is the γ-transmission coefficient. Note that $\mathcal{T}(E_\gamma)$ is a function that depends solely on E_γ. This is based on the generalized Brink hypothesis [55], which is expected to hold in this case since the studied reaction does not involve high temperatures or spins [30,56,57].

A section of the primary coincidence matrix was then selected for the extraction of the NLD and γSF. To ensure that the experimental data truly correspond to statistical γ decay from compound-nucleus states, a minimum excitation energy $E_{x,\mathrm{low}} = 4.4$ MeV was chosen. In order to exclude data corresponding to the γ decay of ^{64}Ni, an upper limit $E_x = 6.08$ MeV was set, close to the neutron separation energy for ^{65}Ni $S_n = 6.098$ MeV. Finally, a lower limit in the γ energy of $E_{\gamma,\mathrm{low}} = 1.6$ MeV was employed.

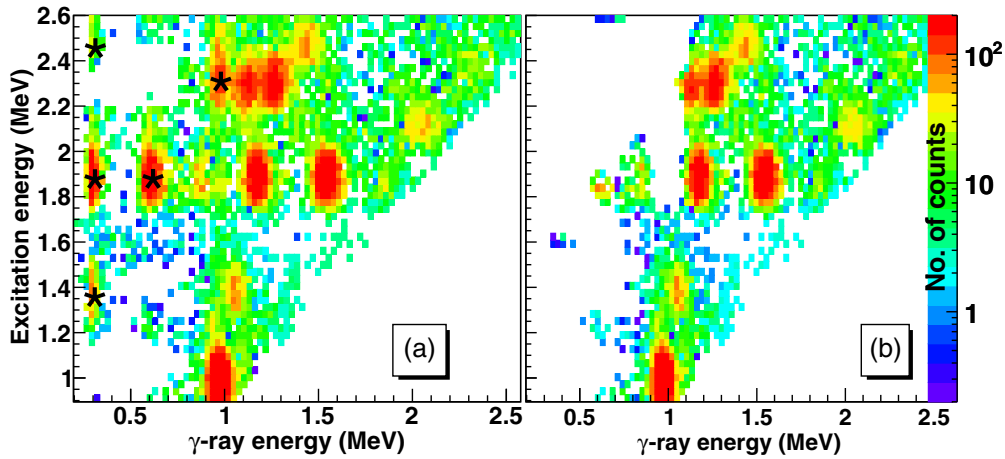

FIG. 3. Section of the unfolded coincidence matrix for ^{65}Ni (a) compared to the first-generation matrix (b). The peaks marked with a $\star$ correspond to removed secondary transitions: for instance, part (a) shows the decay cascade $E_x = 1609 \rightarrow 310 \rightarrow 0$ keV, while in part (b) the secondary transition $310 \rightarrow 0$ keV has been removed and only the peak for the $E_x = 1609 \rightarrow 310$ keV transition is seen.

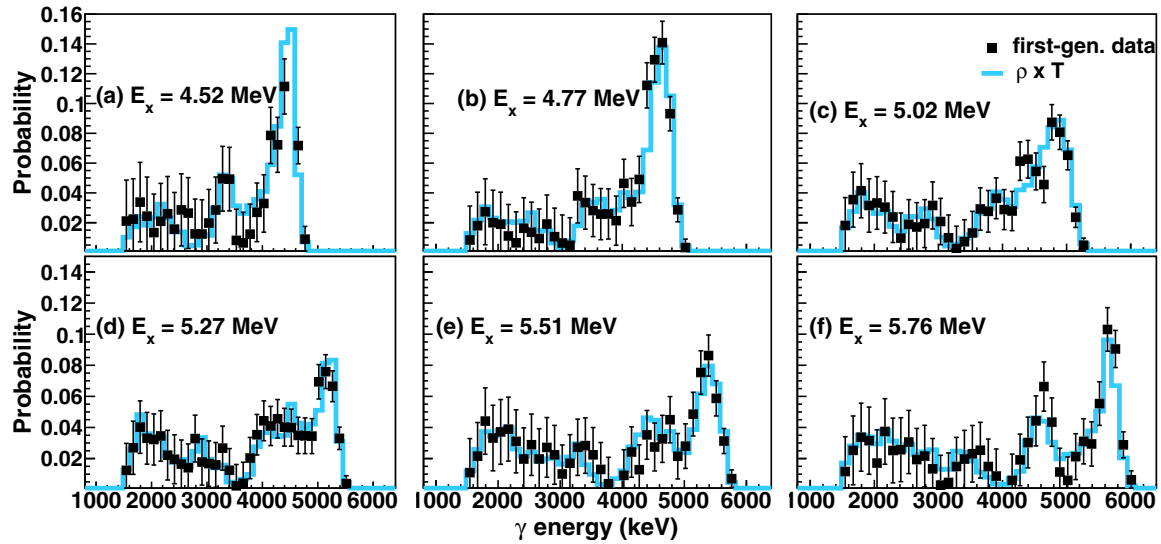

FIG. 4. Comparison between the first-generation matrix for ^{65}Ni projected for a given E_x, and the corresponding product $\rho(E_x - E_\gamma)\mathcal{T}(E_\gamma)$.

As described in detail by Ref. [47], the least-χ^2 fit of $\rho\mathcal{T}$ was calculated, with every point of the functions ρ and $\mathcal{T}$ as an independent variable. A minimum for the χ^2 was reached within 30 iterations, without making any additional assumptions about the functional forms of ρ and $\mathcal{T}$. The result of this fit is a family of functions $\tilde{\rho}(E_x - E_\gamma)$ and $\tilde{\mathcal{T}}(E_\gamma)$ characterized by

$$\tilde{\rho}(E_x - E_\gamma) = \mathscr{A}\exp[\alpha(E_x - E_\gamma)]\,\rho(E_x - E_\gamma), \quad (2)$$

$$\tilde{\mathcal{T}}(E_\gamma) = \mathscr{B}\exp(\alpha E_\gamma)\mathcal{T}(E_\gamma), \quad (3)$$

where, if $\rho(E_x - E_\gamma)$ and $\mathcal{T}(E_\gamma)$ are the solutions of a fit to a given set of experimental data, $\tilde{\rho}(E_x - E_\gamma)$ and $\tilde{\mathcal{T}}(E_\gamma)$ would give identical fits, as proven in Ref. [47]. Figure 4 shows a comparison between the first-generation matrix projected for a given excitation energy bin and the corresponding product $\rho(E_x - E_\gamma)\mathcal{T}(E_\gamma)$. The agreement expected from Eq. (1) is clearly seen in all cases, indicating that the functional dependence of the NLD and the γ-transmission coefficient has been successfully extracted over the whole excitation energy range considered.

Once the functional form of ρ and $\mathcal{T}$ was obtained, the physical solution, given by a particular set of transformation parameters $\mathscr{A}$, α, and $\mathscr{B}$, was determined by normalization to additional experimental data. From the normalized $\mathcal{T}(E_\gamma)$, the γ-strength function $f_L(E_\gamma)$ was obtained with the relation [58,59]

$$f_L(E_\gamma) = \frac{\mathcal{T}(E_\gamma)}{2\pi E_\gamma^{2L+1}}, \quad (4)$$

where L is the multipolarity of the transition, here taken as $L = 1$ since dipole radiation represents the main contribution to the γSF, as supported by experimental data [32,59]. The normalization procedures for the NLD and γSF are described in the following section.

III. NORMALIZATION OF THE NUCLEAR LEVEL DENSITY AND THE γ-STRENGTH FUNCTION

A. Nuclear level density

For the normalization of the NLD, discrete energy levels from Ref. [52] were used together with an estimated value of the NLD at the neutron separation energy, $\rho(S_n)$. At excitation energies below $E_x \approx 3$ MeV, where the level scheme of ^{65}Ni is regarded to be complete [60], the normalization was performed by requiring a good agreement (within the error bars) between the cumulative number of levels in the experimental NLD and the tabulated values from Ref. [52]. In addition, a good agreement between the experimental NLD at $E_x \approx 3$ MeV and the value of $\rho(S_n)$ was required. Assuming that both positive and negative parity states contribute equally to the NLD (parity symmetry) and considering the standard spin distribution [61,62]

$$g(E_x, I) \simeq \frac{2I+1}{2\sigma^2}\exp[-(I+1/2)^2/2\sigma^2] \quad (5)$$

for a specific excitation energy E_x, spin I, and a spin cutoff parameter σ, the value of $\rho(S_n)$ was obtained through the relation [47]

$$\rho(S_n) = \frac{2\sigma^2}{D_0}\frac{1}{(I_t+1)\exp[-(I_t+1)^2/2\sigma^2] + I_t\exp\left[-I_t^2/2\sigma^2\right]}, \quad (6)$$

where D_0 is the level spacing of s-wave resonances and I_t is the ground-state spin of the target nucleus in the (n,γ) reaction, i.e, 0^+ for ^{64}Ni.

The σ parameter was determined within the backshifted Fermi gas (BSFG) model with parameters from Ref. [63]:

$$\sigma^2(E_x) = 0.391A^{0.675}(E_x - 0.5E_{Pa'})^{0.312}, \quad (7)$$

where A is the mass number of the nucleus and $E_{Pa'}$ is the deuteron pairing energy. The resulting $\sigma = 3.37$ was used together with a parameter $D_0 = 21200 \pm 2000$ eV [64]. The

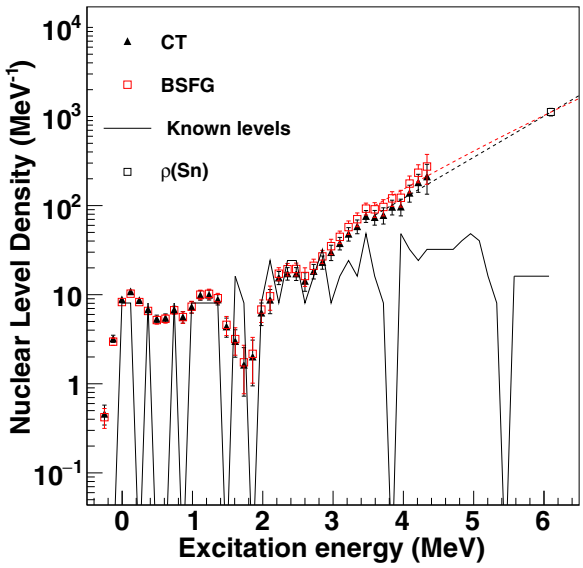

FIG. 5. Normalized NLD for ^{65}Ni using the CT model and the BSFG model for interpolation between the experimental data obtained in this work and the estimated value of $\rho(S_n)$. The bin width is 124 keV.

obtained NLD at S_n, assuming parity symmetry, is $\rho(S_n) = 1124(106)\ \mathrm{MeV}^{-1}$.

With the Oslo method described in Sec. II, the functional form of the NLD is extracted up to $E_x \approx S_n - E_{\gamma,\mathrm{low}}$. Therefore, an interpolation between the experimental data from this work and the value of $\rho(S_n)$ obtained from Eq. (6) was required. For this purpose, two different models for the NLD have been considered: the constant temperature (CT) model [61,65] and the BSFG model [65]. The CT model describes the NLD as

$$\rho(E_x) = \frac{1}{T}\exp\frac{E_x - E_0}{T}, \tag{8}$$

where E_0 is the energy backshift and T is the nuclear temperature parameter. By requiring agreement between the NLD at $E_x \approx 3$ MeV and $\rho(S_n)$, the values $E_0 = -0.44 \pm 0.08$ MeV and $T = 0.94 \pm 0.02$ MeV were obtained, in accordance with the values suggested by Ref. [63], $E_0^{EB} = -0.67 \pm 0.47$ MeV and $T^{EB} = 0.96 \pm 0.07$ MeV.

In a similar manner, the interpolation was performed using the BSFG model, which describes the NLD as [65]

$$\rho(E_x) = \frac{1}{12\sqrt{2}\sigma}\frac{e^{2\sqrt{a(E_x-E_1)}}}{a^{1/4}(E_x-E_1)^{5/4}}, \tag{9}$$

where a is the level density parameter and E_1 is the energy backshift parameter, here $a = 7.77\ \mathrm{MeV}^{-1}$ and $E_1 = -0.17$ MeV, as proposed by Ref. [63].

The normalized level density for ^{65}Ni is depicted in Fig. 5 as obtained with the CT model and the BSFG model interpolations. The results with both interpolations are very similar. All the parameters used for the normalization of the level density are given in Table I.

In Eq. (6) parity symmetry of the NLD is assumed; i.e, the level densities at S_n for positive and negative parity states are considered to contribute equally to $\rho(S_n)$ [47]. However, as detailed in Ref. [48], this is not necessarily the case. For this reason, the effect of parity asymmetry has been tested here. Defining the parity asymmetry coefficient ζ [66],

$$\zeta = \frac{\rho_+ - \rho_-}{\rho_+ + \rho_-}, \tag{10}$$

with ρ_+ and ρ_- the positive and negative parity level densities, the NLD at S_n including parity asymmetry $\rho_\zeta(S_n)$ can be expressed as

$$\rho_\zeta(S_n) = \frac{2\sigma^2}{D_0(1-\zeta)}\frac{1}{(I_t+1)\exp\left[-\frac{(I_t+1)^2}{2\sigma^2}\right] + I_t\exp\left[-\frac{(I_t)^2}{2\sigma^2}\right]}. \tag{11}$$

Using microscopic calculations from Ref. [67], a value $\zeta \simeq -0.07$ at $E_x = S_n$ was obtained, resulting in $\rho_\zeta(S_n) = 1210(120)\ \mathrm{MeV}^{-1}$. The effect of parity asymmetry in the NLD at S_n is therefore small for the present case, $\rho_\zeta(S_n)$ being less than 8% higher than the value for which parity asymmetry is neglected and within its estimated error bar. This is in agreement with the results for other Ni isotopes such as ^{58}Ni [68] and ^{64}Ni [37].

B. γ-strength function

Once the slope of the NLD was obtained (parameter α), the absolute normalization of the γSF was determined (parameter $\mathscr{B}$). This was done using known values of the average, total radiative width at S_n, $\langle\Gamma_{\gamma 0}\rangle$, extracted from s-wave neutron resonances [69]:

$$\begin{aligned}\langle\Gamma_\gamma(S_n, I_t \pm 1/2, \pi_t)\rangle &= \frac{D_0}{4\pi}\int_{E_\gamma=0}^{S_n} dE_\gamma \mathscr{B}\mathscr{T}(E_\gamma) \\ &\times \rho(S_n - E_\gamma)\sum_{I=-1}^{1} g(S_n - E_\gamma, I_t \pm 1/2 + I),\end{aligned} \tag{12}$$

where I_t and π_t are the ground state spin and parity of the target nucleus in the (n,γ) reaction, $\rho(S_n - E_\gamma)$ is the experimental level density and, g is the spin distribution given by Eq. (5). Only two resonances were available in Ref. [64] for ^{65}Ni, with $\langle\Gamma_{\gamma,0}\rangle = 1010 \pm 70$ MeV and $\langle\Gamma_{\gamma,0}\rangle = 1160 \pm 80$ MeV, for incident neutron energies of 14.3 and 33.8 keV, respectively. A

TABLE I. Parameters used to normalize the level density of ^{65}Ni (see text).

$\sigma(S_n)$	D_0 (10^3 eV)	T (MeV)	E_0 (MeV)	a (MeV^{-1})	E_1 (MeV)	$\rho(S_n)$ ($10^3\ \mathrm{MeV}^{-1}$)	$\rho_\zeta(S_n)$ ($10^3\ \mathrm{MeV}^{-1}$)
3.52	21.10 ± 2.00	0.94(0.02)	−0.44(0.08)	7.77	−0.17	1.12(11)	1.21(12)

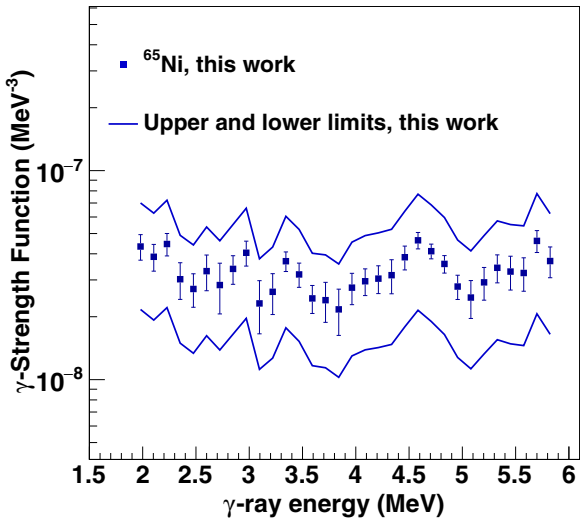

FIG. 6. The γSF of ^{65}Ni together with its upper and lower limits. The error bars include statistical uncertainties plus systematic errors from the unfolding and extraction of the primary γ rays.

value $\langle\Gamma_{\gamma,0}\rangle = 1085$ MeV was used, obtained as the average of the two resonances. The normalized γSF of ^{65}Ni obtained in this work is shown in Fig. 6. The upper and lower limits for the γSF were also determined, taking into account the uncertainties in both the α and $\mathscr{B}$ parameters. For this purpose, the effect of parity and the unknown $E1/M1$ composition of the γSF were also considered and estimated using the program TALYS [70]. As a result, an global uncertainty of $\approx$50% was obtained for the absolute normalization of the γSF, corresponding to $\langle\Gamma_{\gamma,0}\rangle = 1085 \pm 550$ MeV. The shape of the γSF is obtained from the normalization of the NLD and it is therefore not dependent on the chosen value of $\langle\Gamma_{\gamma,0}\rangle$. A different choice of $\langle\Gamma_{\gamma,0}\rangle$ would result in a different absolute normalization of the γSF, but would not affect its overall shape.

IV. REGIMES OF γ DECAY

A. γ decay at low excitation energies

The particle-γ coincidences analyzed in this work have also been used to study the γ decay of ^{65}Ni from low excitation energies (below $\approx$4 MeV). Several γ-ray transitions tabulated in Ref. [52] can be identified in the coincidence matrices displayed in Figs. 1 and 3. Further, other γ-ray lines not listed in Ref. [52] have been observed in this work. In particular, a peak at $(E_x, E_\gamma) \approx (1920, 1210)$ keV has been seen, corresponding to the primary transition $E_x = 1920 \rightarrow 693$ keV, of tentative $E1$ character according to the spin-parity assignments given in Ref. [52]. The subsequent secondary decay from $E_x = 693$ keV is seen as a peak at $(E_x, E_\gamma) \approx (1920, 630)$ keV in the unfolded matrix.

In addition, the primary coincidence matrix displays peaks at $(E_x, E_\gamma) \approx (2320, 1290)$ keV and $(E_x, E_\gamma) \approx (2320, 1150)$ keV, which could correspond to the decay of the tabulated levels at $E_x = 2302, 2324.7, 2336$ keV into the states at $E_x = 1017.01$ keV and $E_x = 1141.7$ keV, respectively. A clear peak at $(E_x, E_\gamma) \approx (2480, 1460)$ keV is also observed, corresponding to a primary transition to the fourth excited state at $E_x = 1017.01$ keV. Further, strong primary transitions are measured from $E_x \approx 2790$ keV to the levels at $E_x = 63, 310$ and 693 keV. Above $E_x \approx 3$ MeV, the presence of two strong, broad peaks at $(E_x, E_\gamma) \approx (3340, 3020)$ keV and $(E_x, E_\gamma) \approx (3530, 3220)$ keV indicates a strong feeding of the $E_x = 310$ keV state from several energy levels in the interval $E_x \approx 3.2$–3.5 MeV. The results presented in this section are summarized in Table II and displayed in Fig. 7.

TABLE II. Some of the primary γ-ray transitions observed in this work. The resolution is given as FWHM.

E_i (keV)	E_f (keV)	E_γ (keV)
1920	693	1210 (90)
2300	1141	1150 (80)
2300	1017	1290 (100)
2480	1017	1460 (100)
2790	0–63	2740 (180)
2790	310	2490 (160)
2790	693	2100 (150)
3340	310	3020 (200)
3530	310	3220 (210)

B. Compound versus direct nuclear γ decay

As detailed in Sec. II, the Oslo method is based on the hypothesis of statistical γ decay. For this reason, only a region of the particle-γ coincidence matrix was selected by choosing the limits $E_{x,\mathrm{low}}$, $E_{x,\mathrm{up}}$, and $E_{\gamma,\mathrm{low}}$, as shown in Fig. 8. Even though the selected region contains a large, smooth area of coincidences, a strong diagonal at $E_x \approx E_\gamma$ can be

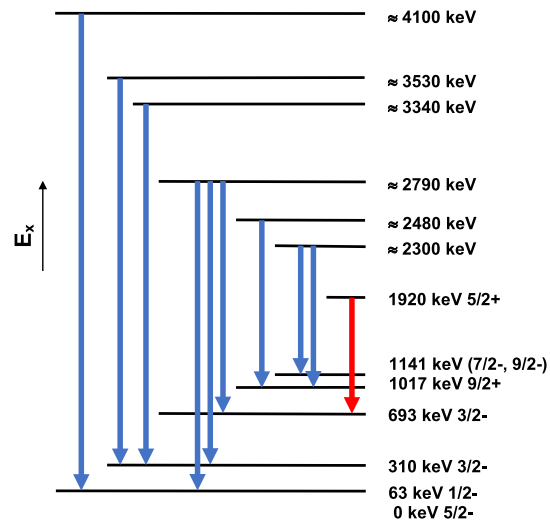

FIG. 7. Partial level scheme with some of the primary γ-ray transitions observed in this work. The $E_x = 1920 \rightarrow 693$ keV primary transition, of tentative $E1$ character according to the spin-parity assignments from Ref. [52], is marked in red. Note that the width of the arrows is not related to the decay intensities.

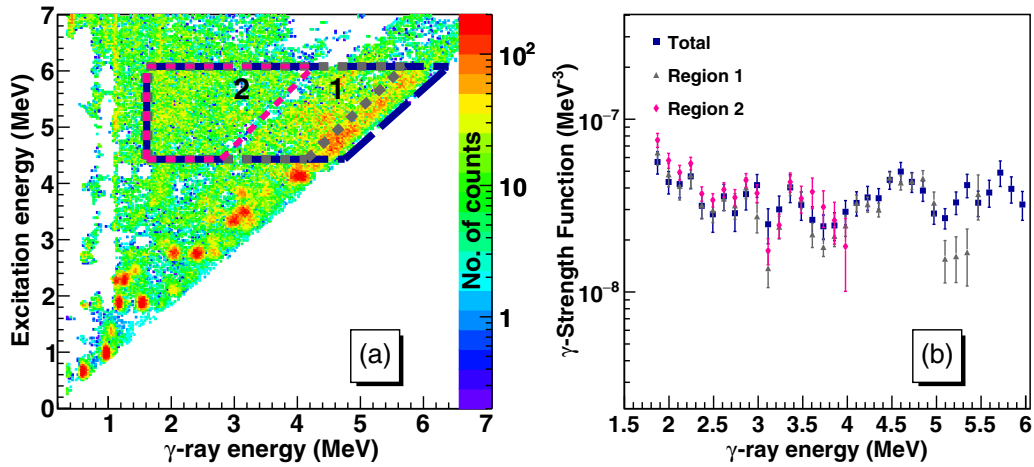

FIG. 8. γSF as obtained from different regions in the first-generation coincidence matrix. Part (a) shows the considered regions in the coincidence matrix while part (b) shows the resulting γSF. The total region corresponds to the standard γSF as detailed in Sec. III B.

clearly seen, indicating the presence of strong, direct γ-ray transitions feeding both the ground state, $I^\pi = 5/2^-$, and the first excited state at 63.37 keV, $I^\pi = 1/2^-$. Since the S_n for ^{65}Ni is considerably lower than for its neighboring nuclei, these direct, nonstatistical γ-decay transitions are strong even at excitation energies very close to S_n.

In order to study the impact of these transitions in the γSF, the Oslo method has been applied to smaller and smoother regions of the first-generation coincidence matrix, as depicted in Fig. 8. The strong diagonal at $E_x \approx E_\gamma$ has been excluded in region 1. The resulting γSF is displayed in Fig. 8 and compared with the results from Sec. III B (standard). Further, a smaller section of the matrix (region 2) has been selected and the corresponding γSF has been included in Fig. 8. It should be noted that region 2 does not present any strong peaks: it is a very homogeneous section in which the statistical γ decay from compound nuclear states clearly dominates. The resulting γSFs from the three selected regions are in reasonable agreement and well within their error bars. Therefore, despite the presence of direct γ-ray transitions corresponding to the strong diagonal, the obtained total γSF can be considered a reasonable estimate of the γ strength from compound nuclear states, at least for $E_\gamma < 5$ MeV. Above $E_\gamma = 5$ MeV no data can be obtained without including the diagonal, and the strong transitions feeding the ground and first excited states of ^{65}Ni are the ones contributing to the observed strength.

V. DISCUSSION OF THE RESULTS

A. The nuclear level density

As seen in Fig. 5, the structures present in the NLD of ^{65}Ni nicely reproduce the discrete energy levels below $E_x \approx 1.4$ MeV [52]. However, a discrepancy between the experimental NLD and the discrete levels at $E_x \approx 1.6$–1.8 MeV is observed: while Ref. [52] includes levels at $E_x = 1594$ keV and $E_x = 1772$ keV, the experimental NLD obtained in this work drops at these energies, increasing again at $E_x \approx 2$ MeV. In other words, the NLD does not show evidence of these levels, neither does the single-particle spectrum shown in Fig. 9. Further, no presence of these levels is seen in the coincidence matrix displayed in Fig. 1. This indicates that the levels were not populated in this experiment, either directly in the reaction or through γ decay from the quasicontinuum of ^{65}Ni. The considered levels are not observed in Ref. [71] or [72] and the spin-parity assignment for the level at $E_x = 1772$ keV shown in Ref. [52] is only tentative. Therefore, further experiments would be desirable in order to confirm or disprove the presence of the levels at $E_x = 1594$ keV and $E_x = 1772$ keV.

At $E_x \approx 3.4$–3.6 MeV, a step-like structure is seen, which could be related to the breaking of nucleon pairs and/or shell effects. It should be noted that the proton and neutron pairing energies are $\Delta_p = 1854$ keV and $\Delta_n = 1595$ keV for ^{64}Ni, and $\Delta_p = 1322$ keV for ^{65}Ni [1]. In addition, the single-particle energies considered in Ref. [73] for the ^{56}Ni core are 8.624, 5.679, 1.383, and 4.137 MeV for the $f_{7/2}$, $p_{3/2}$, $f_{5/2}$, and $p_{1/2}$ orbits, respectively. This results in an energy gap of ≈2.8 MeV between the $p_{1/2}$ and the $f_{5/2}$ orbits and ≈3.0 MeV between

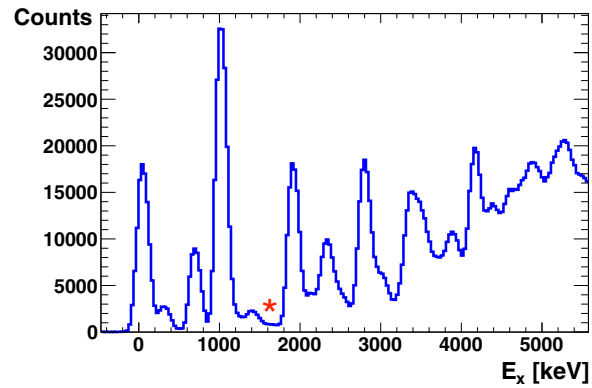

FIG. 9. Experimental excitation energies of ^{65}Ni obtained from single-particle spectra (emitted protons). The ⋆ indicates the excitation energy where the $E_x = 1594$ keV and $E_x = 1772$ keV levels should appear according to Ref. [52]. No evidence for these levels was found in the present work.

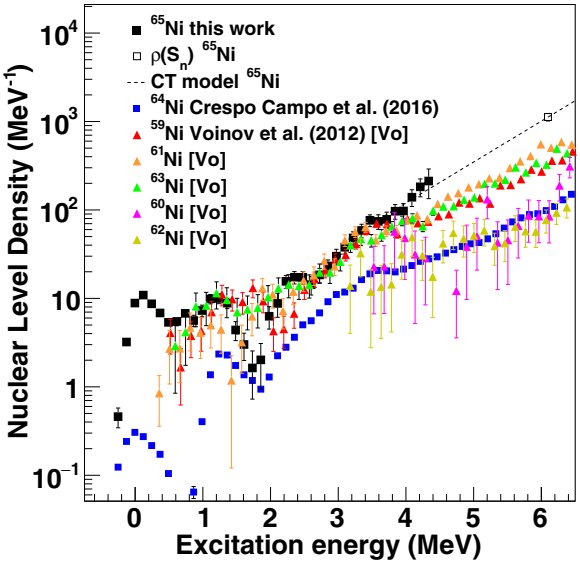

FIG. 10. The NLD of ^{65}Ni compared to the results for ^{64}Ni [37] and the NLD of $^{59-63}$Ni given by Ref. [74].

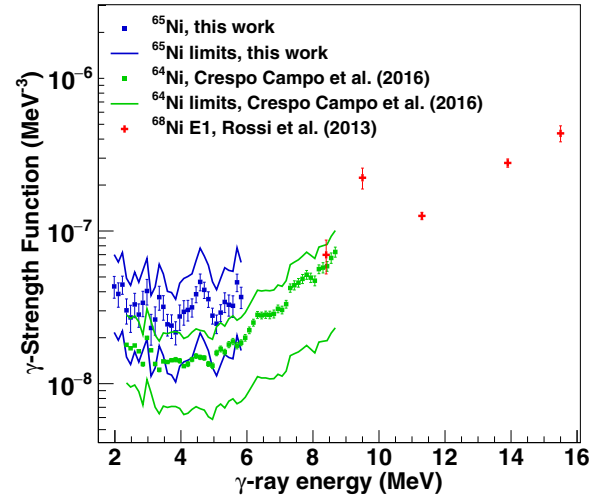

FIG. 11. The γSF of ^{65}Ni obtained in this work compared to the results for ^{64}Ni [37] and ^{68}Ni [29].

the $f_{7/2}$ and the $p_{3/2}$ orbits. Since these values are not far off from the estimates of twice the nucleon pairing energy, it is difficult to determine the contributions from nucleon pair breaking and shell effects to the observed step-like structure.

A comparison of the results from this work and the NLD of other Ni isotopes is shown in Fig. 10. The step-like structure seen in ^{65}Ni at $E_x \approx 3.4$–3.6 MeV is observed at the same energy in the NLD for ^{64}Ni [37]. The results for ^{59,61,63}Ni [74] also show a similar structure at $E_x \approx 3.4$–3.7 MeV. The NLD of ^{65}Ni is very similar to the results for ^{59,61,63}Ni up to $E_x \approx 4$ MeV. Above this energy, the NLD of ^{65}Ni is higher than for the other Ni isotopes displayed in Fig. 10. This is consistent with the available D_0 values for the Ni isotopes [60,64] as well as with the NLD parameters suggested by Ref. [63]: within the CT model, the T parameter for ^{65}Ni is considerably lower than for $^{59-63}$Ni, suggesting a steeper slope for the NLD of the former.

Finally, the overall difference between the experimental data for even- and odd-A Ni isotopes is clearly seen in Fig. 10: the NLD is higher for the odd-A Ni isotopes all over the displayed excitation energy range, being a factor of 3–4 times higher than for the even-A isotopes at $E_x \approx 4$ MeV. This effect is now generally well understood [75,76], being very likely related to the valence hole for the case of ^{65}Ni.

B. The γ-strength function

The γSF of ^{65}Ni displays additional strength with respect to the low-energy tail of the GDR.[2] Whether this additional strength is $E1$, $M1$, or a mixture of both has not been determined in this work. Below $E_\gamma \approx 3$ MeV, a low-energy enhancement is observed in agreement with the experimental results for other Ni isotopes such as ^{60}Ni [40] and ^{64}Ni [37]. Figure 11 shows a comparison between the γSF of ^{65}Ni obtained in this work and the results for ^{64}Ni [37] and ^{68}Ni [29]. The upbend in the γSF of ^{65}Ni is comparable to the observations for ^{64}Ni, despite the differences in the absolute values for both cases. As commented in Sec. III B, the shape of the γSF does not depend on its absolute normalization and therefore the presence of the low-energy enhancement in the results from this work is independent of the chosen value of $\langle\Gamma_{\gamma,0}\rangle$.

In addition, a resonance-like structure is seen at $E_\gamma \simeq 4.6$ MeV. If found to be of $E1$ character, it could correspond to a pygmy resonance (see Sec. I). However, this type of resonance is most often seen closer to the neutron separation energy, as is the case for ^{68}Ni [29]. On the other hand, the measured structure could also correspond to accumulation of $M1$ strength, seen at higher energies is other Ni isotopes: as shown in Ref. [24], a spin-flip resonance has been measured at $E_x \approx 8$–9 MeV in ^{60}Ni [24], while the results from Ref. [25], indicate the presence of resonances with a significant $M1$ component at $E_\gamma \approx 9$–14 MeV in ^{58,60,62}Ni.

In addition to the structure seen at $E_\gamma \simeq 4.6$ MeV, an accumulation of strength at $E_\gamma \simeq 2.6$–3.6 MeV is observed, possibly also a resonance. If the presence of this resonance was confirmed and found to be of $M1$ character, it would likely contain contributions from a scissors mode, expected to be at $E_\gamma \simeq 2$–3 MeV, based on the deformation for neighboring Ni isotopes [52]. Finally, the experimental γSF suggests the presence of additional strength with respect to the GDR close to S_n, as also seen for ^{64}Ni [37]. However, as explained in Sec. IV B, whether this strength represents a resonance or is just the result of strong direct γ decay feeding the ground and first excited states could not be determined in the present work.

VI. SUMMARY AND OUTLOOK

The γ decay of ^{65}Ni has been studied from particle-γ coincidence data on the ^{64}Ni$(d,p\gamma)^{65}$Ni reaction. At excitation energies < 4 MeV, several γ-ray transitions tabulated in

[2]See Ref. [37] for an estimation of the GDR strength in ^{64}Ni within a Generalized Lorentzian model [60].

Ref. [52] have been observed, in addition to a primary 1920 → 693 keV transition not included in Ref. [52].

The particle-γ coincidences have been analyzed through the Oslo method. The shapes of the NLD and γSF of ^{65}Ni have been constrained and the robustness of the Oslo method has been illustrated. The level density of ^{65}Ni is in good agreement with known levels at low excitation energy except for those at $E_x \approx 1.6$–1.8 MeV, for which no experimental evidence has been found in the present work. As previously seen for ^{64}Ni, a step-like structure in the NLD is measured at $E_x \approx 3.4$–3.6 MeV, most likely related to the breaking of nucleon pairs and/or shell effects.

The γSF suggests an enhancement or upbend below $E_\gamma \approx 3$ MeV, comparable with the results for ^{60}Ni and ^{64}Ni obtained in other works. A resonance-like structure is seen at 4.6 MeV as well as some additional strength at $E_x \approx 2.6$–3.6 MeV. Further experiments to determine the electromagnetic character of this strength would be of great value.

The obtained results contribute to the systematic study of the upbend and γ resonances in the Ni isotopes, manifestations of complex nuclear structure phenomena that remain to be fully understood.

ACKNOWLEDGMENTS

We would like to thank INFN Laboratory Nazionali di Legnaro for providing the ^{64}Ni target. We are also grateful for the financial support received from the Research Council of Norway (NFR). A.C.L. acknowledges funding from the ERC-STG-2014 under Grant Agreement No. 637686. S.S. acknowledges financial support by the NFR under Project Grant No. 210007 and G.M.T. acknowledges support under Grant No. 222287. Finally, we would like to specially thank J. C. Müller, A. Semchenkov, and J. Wikne for providing the beam for our experiment.

[1] A. Bohr and B. Mottelson, *Nuclear Structure* (Benjamin, New York, 1969), Vol. I.

[2] A. Bohr and B. Mottelson, *Nuclear Structure* (Benjamin, New York, 1969), Vol. II.

[3] K. Garofali, R. Robinson, and M. Thoennessen, At. Data Nucl. Data Tables **98**, 356 (2012), and references therein.

[4] R. Broda, T. Pawłat, W. Królas, R. V. F. Janssens, S. Zhu, W. B. Walters, B. Fornal, C. J. Chiara, M. P. Carpenter, N. Hoteling, Ł. W. Iskra, F. G. Kondev, T. Lauritsen, D. Seweryniak, I. Stefanescu, X. Wang, and J. Wrzesiński, Phys. Rev. C **86**, 064312 (2012), and references therein.

[5] J. P. Schiffer, C. R. Hoffman, B. P. Kay, J. A. Clark, C. M. Deibel, S. J. Freeman, M. Honma, A. M. Howard, A. J. Mitchell, T. Otsuka, P. D. Parker, D. K. Sharp, and J. S. Thomas, Phys. Rev. C **87**, 034306 (2013).

[6] D. Rudolph, C. Baktash, M. J. Brinkman, E. Caurier, D. J. Dean, M. Devlin, J. Dobaczewski, P.-H. Heenen, H.-Q. Jin, D. R. LaFosse, W. Nazarewicz, F. Nowacki, A. Poves, L. L. Riedinger, D. G. Sarantites, W. Satuła, and C.-H. Yu, Phys. Rev. Lett. **82**, 3763 (1999).

[7] D. Rudolph, I. Ragnarsson, W. Reviol, C. Andreoiu, M. A. Bentley, M. P. Carpenter, R. J. Charity, R. M. Clark, M. Cromaz, J. Ekman, C. Fahlander, P. Fallon, E. Ideguchi, A. O. Macchiavelli, M. N. Mineva, D. G. Sarantites, D. Seweryniak, and S. J. Williams, J. Phys. G: Nucl. Part. Phys. **37**, 075105 (2010).

[8] E. K. Johansson, D. Rudolph, I. Ragnarsson, L.-L. Andersson, D. A. Torres, C. Andreoiu, C. Baktash, M. P. Carpenter, R. J. Charity, C. J. Chiara, J. Ekman, C. Fahlander, O. L. Pechenaya, W. Reviol, R. du Rietz, D. G. Sarantites, D. Seweryniak, L. G. Sobotka, C. H. Yu, and S. Zhu, Phys. Rev. C **80**, 014321 (2009).

[9] D. A. Torres, F. Cristancho, L.-L. Andersson, E. K. Johansson, D. Rudolph, C. Fahlander, J. Ekman, R. du Rietz, C. Andreoiu, M. P. Carpenter, D. Seweryniak, S. Zhu, R. J. Charity, C. J. Chiara, C. Hoel, O. L. Pechenaya, W. Reviol, D. G. Sarantites, L. G. Sobotka, C. Baktash, C.-H. Yu, B. G. Carlsson, and I. Ragnarsson, Phys. Rev. C **78**, 054318 (2008).

[10] M. Albers, S. Zhu, R. V. F. Janssens, J. Gellanki, I. Ragnarsson, M. Alcorta, T. Baugher, P. F. Bertone, M. P. Carpenter, C. J. Chiara, P. Chowdhury, A. N. Deacon, A. Gade, B. DiGiovine, C. R. Hoffman, F. G. Kondev, T. Lauritsen, C. J. Lister, E. A. McCutchan, D. S. Moerland, C. Nair, A. M. Rogers, and D. Seweryniak, Phys. Rev. C **88**, 054314 (2013).

[11] M. Albers, S. Zhu, A. D. Ayangeakaa, R. V. F. Janssens, J. Gellanki, I. Ragnarsson, M. Alcorta, T. Baugher, P. F. Bertone, M. P. Carpenter, C. J. Chiara, P. Chowdhury, H. M. David, A. N. Deacon, B. DiGiovine, A. Gade, C. R. Hoffman, F. G. Kondev, T. Lauritsen, C. J. Lister, E. A. McCutchan, C. Nair, A. M. Rogers, and D. Seweryniak, Phys. Rev. C **94**, 034301 (2016).

[12] E. K. Johansson, D. Rudolph, L.-L. Andersson, D. A. Torres, I. Ragnarsson, C. Andreoiu, C. Baktash, M. P. Carpenter, R. J. Charity, C. J. Chiara, J. Ekman, C. Fahlander, C. Hoel, O. L. Pechenaya, W. Reviol, R. du Rietz, D. G. Sarantites, D. Seweryniak, L. G. Sobotka, C. H. Yu, and S. Zhu, Phys. Rev. C **77**, 064316 (2008).

[13] M. Bernas, P. Dessagne, M. Langevin, J. Payet, F. Pougheon, and P. Roussel, Phys. Lett. B **113**, 279 (1982).

[14] O. Sorlin, S. Leenhardt, C. Donzaud, J. Duprat, F. Azaiez, F. Nowacki, H. Grawe, Z. Dombradi, F. Amorini, A. Astier, D. Baiborodin, M. Belleguic, C. Borcea, C. Bourgeois, D. M. Cullen, Z. Dlouhy, E. Dragulescu, M. Gorska, S. Grevy, D. Guillemaud-Mueller, G. Hagemann, B. Herskind, J. Kiener, R. Lemmon, M. Lewitowicz, S. M. Lukyanov, P. Mayet, F. de Oliveira Santos, D. Pantalica, Y.-E. Penionzhkevich, F. Pougheon, A. Poves, N. Redon, M. G. Saint-Laurent, J. A. Scarpaci, G. Sletten, M. Stanoiu, O. Tarasov, and C. Theisen, Phys. Rev. Lett. **88**, 092501 (2002).

[15] R. Broda, B. Fornal, W. Królas, T. Pawłat, D. Bazzacco, S. Lunardi, C. Rossi-Alvarez, R. Menegazzo, G. de Angelis, P. Bednarczyk, J. Rico, D. De Acuña, P. J. Daly, R. H. Mayer, M. Sferrazza, H. Grawe, K. H. Maier, and R. Schubart, Phys. Rev. Lett. **74**, 868 (1995).

[16] F. Recchia, C. J. Chiara, R. V. F. Janssens, D. Weisshaar, A. Gade, W. B. Walters, M. Albers, M. Alcorta, V. M. Bader, T. Baugher, D. Bazin, J. S. Berryman, P. F. Bertone, B. A. Brown, C. M. Campbell, M. P. Carpenter, J. Chen, H. L. Crawford, H. M. David, D. T. Doherty, C. R. Hoffman, F. G. Kondev, A. Korichi, C. Langer, N. Larson, T. Lauritsen, S. N. Liddick, E. Lunderberg, A. O. Macchiavelli, S. Noji, C. Prokop, A. M. Rogers, D. Seweryniak, S. R. Stroberg, S. Suchyta, S.

Williams, K. Wimmer, and S. Zhu, Phys. Rev. C **88**, 041302(R) (2013).
[17] S. Zhu, R. V. F. Janssens, M. P. Carpenter, C. J. Chiara, R. Broda, B. Fornal, N. Hoteling, W. Królas, T. Lauritsen, T. Pawłat, D. Seweryniak, I. Stefanescu, J. R. Stone, W. B. Walters, X. Wang, and J. Wrzesiński, Phys. Rev. C **85**, 034336 (2012).
[18] S. Suchyta, S. N. Liddick, Y. Tsunoda, T. Otsuka, M. B. Bennett, A. Chemey, M. Honma, N. Larson, C. J. Prokop, S. J. Quinn, N. Shimizu, A. Simon, A. Spyrou, V. Tripathi, Y. Utsuno, and J. M. Von Moss, Phys. Rev. C **89**, 021301(R) (2014).
[19] Y. Tsunoda, T. Otsuka, N. Shimizu, M. Honma, and Y. Utsuno, Phys. Rev. C **89**, 031301(R) (2014).
[20] C. J. Chiara, D. Weisshaar, R. V. F. Janssens, Y. Tsunoda, T. Otsuka, J. L. Harker, W. B. Walters, F. Recchia, M. Albers, M. Alcorta, V. M. Bader, T. Baugher, D. Bazin, J. S. Berryman, P. F. Bertone, C. M. Campbell, M. P. Carpenter, J. Chen, H. L. Crawford, H. M. David, D. T. Doherty, A. Gade, C. R. Hoffman, M. Honma, F. G. Kondev, A. Korichi, C. Langer, N. Larson, T. Lauritsen, S. N. Liddick, E. Lunderberg, A. O. Macchiavelli, S. Noji, C. Prokop, A. M. Rogers, D. Seweryniak, N. Shimizu, S. R. Stroberg, S. Suchyta, Y. Utsuno, S. J. Williams, K. Wimmer, and S. Zhu, Phys. Rev. C **91**, 044309 (2015).
[21] C. J. Prokop, B. P. Crider, S. N. Liddick, A. D. Ayangeakaa, M. P. Carpenter, J. J. Carroll, J. Chen, C. J. Chiara, H. M. David, A. C. Dombos, S. Go, J. Harker, R. V. F. Janssens, N. Larson, T. Lauritsen, R. Lewis, S. J. Quinn, F. Recchia, D. Seweryniak, A. Spyrou, S. Suchyta, W. B. Walters, and S. Zhu, Phys. Rev. C **92**, 061302(R) (2015).
[22] G. A. Bartholomew *et al.*,in *Advances in Nuclear Physics*, edited by M. Baranger and E. Vogt (Plenum, New York, 1973), Vol. 7, p. 229.
[23] B. L. Berman and S. C. Fultz, Rev. Mod. Phys. **47**, 713 (1975).
[24] M. Scheck, V. Yu. Ponomarev, M. Fritzsche, J. Joubert, T. Aumann, J. Beller, J. Isaak, J. H. Kelley, E. Kwan, N. Pietralla, R. Raut, C. Romig, G. Rusev, D. Savran, L. Schorrenberger, K. Sonnabend, A. P. Tonchev, W. Tornow, H. R. Weller, A. Zilges, and M. Zweidinger, Phys. Rev. C **88**, 044304 (2013).
[25] C. Djalali, N. Marty, M. Morlet, A. Willis, J. C. Jourdain, N. Anantaraman, G. M. Crawley, A. Galonsky, and P. Kitching, Nucl. Phys. A **388**, 1 (1982).
[26] Y. Suzuki, K. Ikeda, and H. Sato, Prog. Theor. Phys. **83**, 180 (1990).
[27] P. Van Isacker and M. A. Nagarajan, and D. D. Warner, Phys. Rev. C **45**, R13 (1992).
[28] O. Wieland, A. Bracco, F. Camera, G. Benzoni, N. Blasi, S. Brambilla, F. C. L. Crespi, S. Leoni, B. Million, R. Nicolini, A. Maj, P. Bednarczyk, J. Grebosz, M. Kmiecik, W. Meczynski, J. Styczen, T. Aumann, A. Banu, T. Beck, F. Becker, L. Caceres, P. Doornenbal, H. Emling, J. Gerl, H. Geissel, M. Gorska, O. Kavatsyuk, M. Kavatsyuk, I. Kojouharov, N. Kurz, R. Lozeva, N. Saito, T. Saito, H. Schaffner, H. J. Wollersheim, J. Jolie, P. Reiter, N. Warr, G. deAngelis, A. Gadea, D. Napoli, S. Lenzi, S. Lunardi, D. Balabanski, G. LoBianco, C. Petrache, A. Saltarelli, M. Castoldi, A. Zucchiatti, J. Walker, and A. Bürger, Phys. Rev. Lett. **102**, 092502 (2009).
[29] D. M. Rossi, P. Adrich, F. Aksouh, H. Alvarez-Pol, T. Aumann, J. Benlliure, M. Bohmer, K. Boretzky, E. Casarejos, M. Chartier, A. Chatillon, D. Cortina-Gil, U. Datta Pramanik, H. Emling, O. Ershova, B. Fernandez-Dominguez, H. Geissel, M. Gorska, M. Heil, H. T. Johansson, A. Junghans, A. Kelic-Heil, O. Kiselev, A. Klimkiewicz, J. V. Kratz, R. Krucken, N. Kurz, M. Labiche, T. Le Bleis, R. Lemmon, Y. A. Litvinov, K. Mahata, P. Maierbeck, A. Movsesyan, T. Nilsson, C. Nociforo, R. Palit, S. Paschalis, R. Plag, R. Reifarth, D. Savran, H. Scheit, H. Simon, K. Summerer, A. Wagner, W. Walus, H. Weick, and M. Winkler, Phys. Rev. Lett. **111**, 242503 (2013).
[30] A. Voinov, E. Algin, U. Agvaanluvsan, T. Belgya, R. Chankova, M. Guttormsen, G. E. Mitchell, J. Rekstad, A. Schiller, and S. Siem, Phys. Rev. Lett. **93**, 142504 (2004).
[31] M. Guttormsen, R. Chankova, U. Agvaanluvsan, E. Algin, L. A. Bernstein, F. Ingebretsen, T. Lönnroth, S. Messelt, G. E. Mitchell, J. Rekstad, A. Schiller, S. Siem, A. C. Sunde, A. Voinov, and S. Ødegård, Phys. Rev. C **71**, 044307 (2005).
[32] A. C. Larsen, N. Blasi, A. Bracco, F. Camera, T. K. Eriksen, A. Görgen, M. Guttormsen, T. W. Hagen, S. Leoni, B. Million, H. T. Nyhus, T. Renstrøm, S. J. Rose, I. E. Ruud, S. Siem, T. Tornyi, G. M. Tveten, A. V. Voinov, and M. Wiedeking, Phys. Rev. Lett. **111**, 242504 (2013).
[33] A. C. Larsen, I. E. Ruud, A. Bürger, S. Goriely, M. Guttormsen, A. Görgen, T. W. Hagen, S. Harissopulos, H. T. Nyhus, T. Renstrøm, A. Schiller, S. Siem, G. M. Tveten, A. Voinov, and M. Wiedeking, Phys. Rev. C **89**, 014319 (2014).
[34] A. C. Larsen, M. Guttormsen, R. Chankova, F. Ingebretsen, T. Lönnroth, S. Messelt, J. Rekstad, A. Schiller, S. Siem, N. U. H. Syed, and A. Voinov, Phys. Rev. C **76**, 044303 (2007).
[35] A. Bürger, A. C. Larsen, S. Hilaire, M. Guttormsen, S. Harissopulos, M. Kmiecik, T. Konstantinopoulos, M. Krtička, A. Lagoyannis, T. Lönnroth, K. Mazurek, M. Norrby, H. T. Nyhus, G. Perdikakis, S. Siem, A. Spyrou, and N. U. H. Syed, Phys. Rev. C **85**, 064328 (2012).
[36] A. C. Larsen, R. Chankova, M. Guttormsen, F. Ingebretsen, S. Messelt, J. Rekstad, S. Siem, N. U. H. Syed, S. W. Ødegård, T. Lönnroth, A. Schiller, and A. Voinov, Phys. Rev. C **73**, 064301 (2006).
[37] L. C. Campo, F. L. B. Garrote, T. K. Eriksen, A. Görgen, M. Guttormsen, K. Hadynska-Klek, M. Klintefjord, A. C. Larsen, T. Renstrøm, E. Sahin, S. Siem, A. Springer, T. G. Tornyi, and G. M. Tveten, Phys. Rev. C **94**, 044321 (2016).
[38] B. V. Kheswa, M. Wiedeking, F. Giacoppo, S. Goriely, M. Guttormsen, A. C. Larsen, F. L. B. Garrote, T. K. Eriksen, A. Görgen, T. W. Hagen, P. E. Koehler, M. Klintefjord, H. T. Nyhus, P. Papka, T. Renstrøm, S. Rose, E. Sahin, S. Siem, and T. G. Tornyi, Phys. Lett. B **744**, 268 (2015).
[39] A. Simon, M. Guttormsen, A. C. Larsen, C. W. Beausang, P. Humby, J. T. Burke, R. J. Casperson, R. O. Hughes, T. J. Ross, J. M. Allmond, R. Chyzh, M. Dag, J. Koglin, E. McCleskey, M. McCleskey, S. Ota, and A. Saastamoinen, Phys. Rev. C **93**, 034303 (2016).
[40] A. Voinov, S. M. Grimes, C. R. Brune, M. Guttormsen, A. C. Larsen, T. N. Massey, A. Schiller, and S. Siem, Phys. Rev. C **81**, 024319 (2010).
[41] M. Wiedeking, L. A. Bernstein, M. Krtička, D. L. Bleuel, J. M. Allmond, M. S. Basunia, J. T. Burke, P. Fallon, R. B. Firestone, B. L. Goldblum, R. Hatarik, P. T. Lake, I-Y. Lee, S. R. Lesher, S. Paschalis, M. Petri, L. Phair, and N. D. Scielzo, Phys. Rev. Lett. **108**, 162503 (2012).
[42] E. Litvinova and N. Belov, Phys. Rev. C **88**, 031302(R) (2013).
[43] R. Schwengner, S. Frauendorf, and A. C. Larsen, Phys. Rev. Lett. **111**, 232504 (2013).
[44] B. A. Brown and A. C. Larsen, Phys. Rev. Lett. **113**, 252502 (2014).

[45] M. Guttormsen, T. S. Tveter, L. Bergholt, F. Ingebretsen, and J. Rekstad, Nucl. Instrum. Methods Phys. Res., Sect. A **374**, 371 (1996).
[46] M. Guttormsen, T. Ramsøy, and J. Rekstad, Nucl. Instrum. Methods Phys. Res., Sect. A **255**, 518 (1987).
[47] A. Schiller, L. Bergholt, M. Guttormsen, E. Melby, J. Rekstad, and S. Siem, Nucl. Instrum. Methods Phys. Res., Sect. A **447**, 498 (2000).
[48] A. C. Larsen, M. Guttormsen, M. Krtička, E. Běták, A. Bürger, A. Görgen, H. T. Nyhus, J. Rekstad, A. Schiller, S. Siem, H. K. Toft, G. M. Tveten, A. V. Voinov, and K. Wikan, Phys. Rev. C **83**, 034315 (2011).
[49] A. Spyrou, S. N. Liddick, A. C. Larsen, M. Guttormsen, K. Cooper, A. C. Dombos, D. J. Morrissey, F. Naqvi, G. Perdikakis, S. J. Quinn, T. Renstrøm, J. A. Rodriguez, A. Simon, C. S. Sumithrarachchi, and R. G. T. Zegers, Phys. Rev. Lett. **113**, 232502 (2014).
[50] V. W. Ingeberg, Master's thesis, University of Oslo, 2016 (unpublished).
[51] S. N. Liddick, A. Spyrou, B. P. Crider, F. Naqvi, A. C. Larsen, M. Guttormsen, M. Mumpower, R. Surman, G. Perdikakis, D. L. Bleuel, A. Couture, L. C. Campo, A. C. Dombos, R. Lewis, S. Mosby, S. Nikas, C. J. Prokop, T. Renstrøm, B. Rubio, S. Siem, and S. J. Quinn, Phys. Rev. Lett. **116**, 242502 (2016).
[52] Data extracted using the NNDC On-Line Data Service from the ENSDF database, 2015, http://www.nndc.bnl.gov/ensdf/.
[53] M. Guttormsen, A. Bürger, T. E. Hansen, and N. Lietaer, Nucl. Instrum. Methods Phys. Res., Sect. A **648**, 168 (2011).
[54] M. Guttormsen, A. Ataç, G. Løvhøiden, S. Messelt, T. Ramsøy, J. Rekstad, T. F. Thorsteinsen, T. S. Tveter, and Z. Zelazny, Phys. Scr. T **32**, 54 (1990).
[55] D. M. Brink, Doctoral thesis, Oxford University, 1955 (unpublished).
[56] A. Schiller and M. Thoennessen, At. Data Nucl. Data Tables **93**, 549 (2007).
[57] M. Guttormsen, A. C. Larsen, A. Görgen, T. Renstrøm, S. Siem, T. G. Tornyi, and G. M. Tveten, Phys. Rev. Lett. **116**, 012502 (2016).
[58] T. Belgya *et al.*, *Handbook for Calculations of Nuclear Reaction Data, RIPL-2*, IAEA-TECDOC-1506 (IAEA, Vienna, 2006).
[59] J. Kopecky and M. Uhl, Phys. Rev. C **41**, 1941 (1990).
[60] R. Capote *et al.*, Reference Input Parameter Library, RIPL-3, available online at http://www-nds.iaea.org/RIPL-3/.
[61] T. Ericson, Nucl. Phys. **11**, 481 (1959).
[62] T. Ericson and V. Struzinsky, Nucl. Phys. **8**, 284 (1958); **9**, 689 (1958/1959).
[63] T. von Egidy and D. Bucurescu, Phys. Rev. C **80**, 054310 (2009).
[64] S. Mughabhad, *Atlas of Neutron Resonances*, 5th ed. (Elsevier, New York, 2006).
[65] A. Gilbert and A. G. W. Cameron, Can. J. Phys. **43**, 1446 (1965).
[66] U. Agvaanluvsan, G. E. Mitchell, J. F. Shriner Jr., and M. Pato, Phys. Rev. C **67**, 064608 (2003).
[67] S. Goriely, S. Hilaire, and A. J. Koning, Phys. Rev. C **78**, 064307 (2008).
[68] Y. Kalmykov, C. Ozen, K. Langanke, G. Martínez-Pinedo, P. von Neumann-Cosel, and A. Richter, Phys. Rev. Lett. **99**, 202502 (2007).
[69] A. Voinov, M. Guttormsen, E. Melby, J. Rekstad, A. Schiller, and S. Siem, Phys. Rev. C **63**, 044313 (2001).
[70] A. J. Koning, S. Hilaire and M. C. Duijvestijn, TALYS-1.6, software for simulation of nuclear reactions, http://www.talys.eu/home/; in *Proceedings of the International Conference on Nuclear Data for Science and Technology - ND2007, April 22–27, 2007, Nice, France*, edited by O. Bersillon, F. Gunsing, E. Bauge, R. Jacqmin and S. Leray (EDP Sciences, Paris, 2008), pp. 211–214; A. J. Koning and D. Rochman, Nucl. Data Sheets **113**, 2841 (2012).
[71] I. M. Turkiewicz, P. Beuzit, J. Delaunay, and J. P. Fouan, Nucl. Phys. A **143**, 641 (1970).
[72] R. G. Tee and A. Aspinall, Nucl. Phys. A **98**, 417 (1967).
[73] M. Honma, T. Otsuka, B. A. Brown, and T. Mizusaki, Phys. Rev. C **69**, 034335 (2004).
[74] A. Voinov, S. M. Grimes, C. R. Brune, T. Massey, and A. Schiller, EPJ Web Conf. **21**, 05001 (2012); A. Voinov (private communication).
[75] T. Ericson, Adv. Phys. **9**, 425 (1960).
[76] M. Guttormsen, A. Bagheri, R. Chankova, J. Rekstad, S. Siem, A. Schiller, and A. Voinov, Phys. Rev. C **68**, 064306 (2003).